

STUDY ON KINETIC PARAMETERS CHARACTERISTICS OF PEBBLE BED REACTOR USING HTR-PROTEUS FACILITY

by

ZUHAIR *, *Wahid LUTHFI, SRIYONO, SUWOTO, and Topan SETIADIPURA*

Research Center for Nuclear Reactor Technology ORTN – BRIN
Puspittek Area, Serpong, Tangerang Selatan, Indonesia

Scientific paper
<https://doi.org/10.2298/NTRP2202119Z>

The inherent safety feature of a pebble-bed reactor can be observed from its kinetic parameters. Proper modeling for calculating the reactor kinetic is also a concern for safe operation during normal and transient conditions. This study is intended to investigate the kinetic parameters characteristics of a pebble bed reactor using HTR-Proteus. A series of calculations were conducted using MCNP6 code and ENDF/B-VII library. The calculation results show that the negative value on core temperature reactivity is affected dominantly by the Doppler broadening effect. Prompt neutron lifetime ℓ and mean generation time are slightly changed due to an increase in fuel temperature, moderator, and reflector that changed the neutron moderation and absorption over this part of the reactor. For (Th, U)O₂, UO₂, and PuO₂ cores, the effective delayed neutron fraction β_{eff} values are more influenced by ²³³U, ²³⁵U, and ²³⁹Pu, respectively. In terms of stability during reactivity insertion, the UO₂ core is more stable and easier to control because its β_{eff} value is the largest compared to (Th, U)O₂ and PuO₂ cores. It can be concluded that changing temperature must be controlled because it does not only affect the reactivity but also kinetic parameters as part of developing inherent safety features on the pebble-bed reactor.

Key words: kinetic parameter, pebble bed reactor, HTR-proteus, MCNP6, ENDF/B-VII

INTRODUCTION

The increase in world population is predicted to double global energy demand by 2050. Traditional energy sources from fossil fuels such as oil, natural gas, and coal still provide the largest share of the world's energy today. However, fossil fuel is the main contributor to carbon emissions which causes climate change and endangers the world population present and future. Meanwhile, generating energy through nuclear power emits a small amount of CO₂, thus making it a promising option as a solid and reliable energy generation [1]. Since 2000, the Generation IV International Forum (GIF) has conducted a lot of effort in international collaboration to develop next-generation nuclear energy systems. The GIF has provided the basis for identifying and selecting six nuclear energy systems for further research and development of the Generation IV reactor. The Generation IV reactor is expected to be available for commercial deployment around 2030 with more efficient fuel utilization, less waste generation, being economically competitive, and could meet the requirement for safety and proliferation resistance [2].

The pebble bed reactor, a type of high temperature gas-cooled reactor, is one of the six types of Generation IV nuclear reactors with graphite moderator and helium coolant. This reactor is an attractive choice for nuclear energy production due to several advantages, such as the inherent safety features characterized by a strong negative temperature coefficient of reactivity, large thermal inertia from the large graphite mass of the core, and the fuel designed to retain all fission products within the tri-structural isotropic (TRISO) coated particles. These advantages ensure that core meltdown is impossible, and the core remains intact in any accident scenario that causes the reactor temperature increases up to 1600 °C [3]. The pebble bed reactor possesses the flexibility to utilize various fuel cycles, including thorium [4-6], plutonium [7-9], and rock-like oxide [10].

The inherent safety feature of the pebble-bed reactor depends on the calculated kinetic parameters. Accurate calculation of the reactor kinetic is the main concern for safe operation and transient analysis [11]. The purpose of this study is to investigate the characteristics of kinetic parameters for pebble bed reactors using HTR-Proteus [12]. A series of calculations with various temperatures were performed by using the Monte Carlo transport code MCNP6 [13] and the con-

* Corresponding author; e-mail: zuha001@brin.go.id

tinuous energy nuclear data library ENDF/B-VII [14]. The calculation of reactor kinetic parameters was conducted in the configuration of core 4.1 with a fuel-to-moderator pebble ratio of 1:1. Three fuel options for the design consisting of UO_2 , PuO_2 , and $(\text{Th}, \text{U})\text{O}_2$ were adopted to present the calculation inter-comparison of kinetic parameters of pebble bed reactor between uranium, thorium, and plutonium cores. The analysis was performed in the core safety aspect because it can affect the behavior of transients in fatal accident situations.

THE HTR-PROTEUS FACILITY

Proteus is a zero-power research reactor located in the Paul Scherrer Institute, Switzerland. The basic geometry of Proteus consists of a cylindrical graphite annulus with a central cylindrical cavity. The graphite annulus is essentially unchanged for all experimental programs, but the contents of the central cavity can be replaced to adjust the type of reactor to be investigated. Proteus has represented light water reactors throughout its operational history, but from 1992 to 1996, Proteus was configured as a pebble bed reactor critical facility. Consequently, it was denominated as the HTR-Proteus. During this period, seventeen critical assemblies were configured and various experiments of nuclear reactor physics were performed such as criticality, differential, and integral control rod and safety rod worth, kinetics, reaction rates, water ingress effects, and small sample reactivity effects [15].

The HTR-Proteus was constructed to increase confidence in predicting the neutronic behavior of high-temperature gas-cooled reactors. The reactor program was conducted in HTR-Proteus to provide experimental benchmark data. The computational models were reviewed and investigated as a part of the HTR-Proteus program. The integral data obtained from the experimental benchmarking program is intended to validate various physics methods for pebble bed reactor core designs.

The HTR-Proteus facility is cylindrical graphite of 3.262 m in diameter and 3.3 m in height, with a central cylindrical cavity. This cavity has a diameter of 1.25 m and a height of 1.764 m, located 0.78 m above the lower axial reflector. The pulsed neutron source is placed on the bottom of the lower axial reflector. Symmetrically located 160 borings with a diameter of 2.743 cm are also on the lower axial reflector, where at least 127 borings are filled with 2.65 cm diameter graphite rods.

Meanwhile, the upper axial reflector is placed above the core cavity, suspended. It extends beyond the top of the radial reflector. This part is made of a complex structure consisting of graphite, steel, and aluminum as well as including inner and outer aluminum tanks, an aluminum safety ring to prevent the re-

flector from falling onto the pebble bed core during an accident, and a steel lid, support plate, and flanges.

The radial reflector starts from the radial boundary of the core cavity and extends to the outer radial boundary of the reflector, from the bottom of the reflector expanding upwards to a height of 330.4 cm. In this reflector, there is a reactor shutdown and control system, consisting of symmetrically located four boron-steel shutdown rods around the core at a radius of 68.4 cm, and 4 stainless-steel control rods with a radius of 90.6 cm. A schematic top and side view of the HTR-Proteus facility is shown in figs. 1 and 2, respectively.

Loading the HTR-Proteus core is carried out by dropping fuel pebbles into the core through a loading tube suspended above the core. Each fuel pebble is formed by a 5 cm diameter fueled zone and a graphite shell with a thickness of 0.5 cm. The moderator pebbles made of pure graphite with the same diameter as fuel pebbles are also simultaneously dropped in specified proportion to the fuel pebbles. The HTR-Proteus core configuration has different packing fractions because the pebbles are loaded in different ways. In core 4.1 fuel pebble and moderator pebble are loaded in parallel where each pebble is entered into the core from its respective channel. The second method is used for core loading of 4.2 and 4.3 where the fuel pebble and moderator pebble are entered in combination through the same channel. The pebble bed is then flattened after each loading step is completed and the height of the pebble bed core is measured. In the calculation of kinetic parameters, the configuration of core 4.1 was chosen with a fuel and moderator pebbles ratio of 1:1 [17].

In this study, the fueled zone is filled with 15 000 TRISO coated particles dispersed within the graphite matrix. The TRISO coated particles consist of a UO_2 fuel kernel with 18.4% ^{235}U enrichment and four coat-

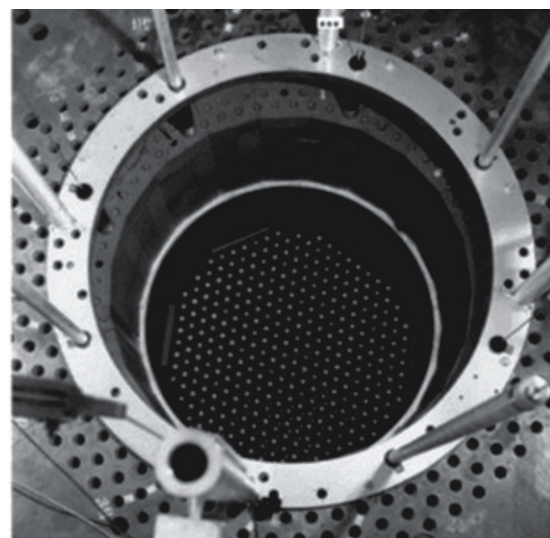


Figure 1. Top view of an HTR-Proteus deterministic core [16]

Figure 2. Schematic side view of the HTR-Proteus facility (dimensions in mm) [16]

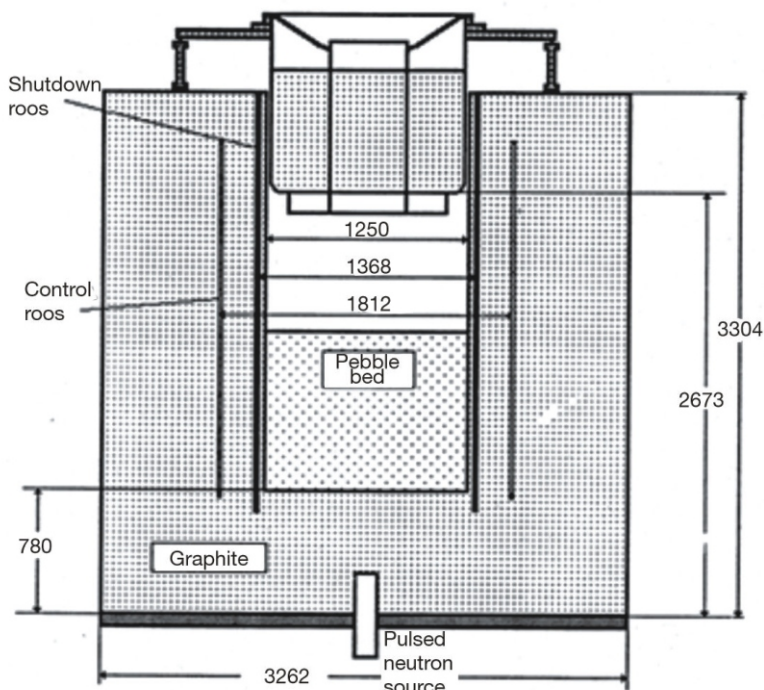
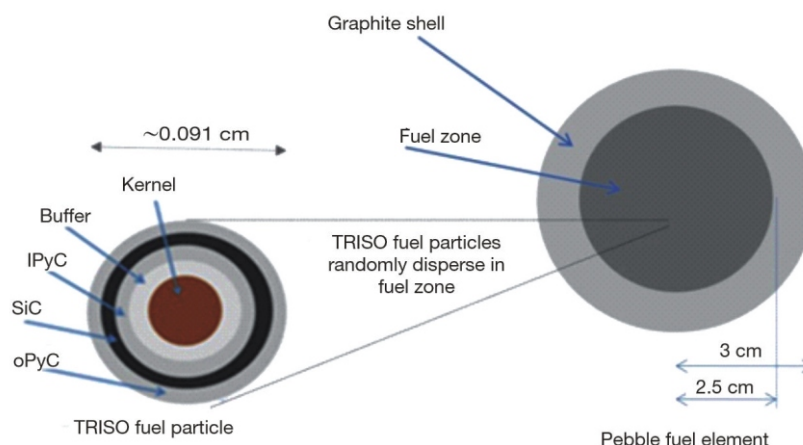


Figure 3. Schematic view of a fuel pebble and a TRISO particle [18]



ing layers. Other TRISO coated particles are formed by (Th,U)O₂ kernel with 12.48% ²³³U enrichment and PuO₂ kernel with plutonium isotopic vector of 0.0259/0.5385/0.2366/0.1313/0.0677 corresponding to plutonium isotopes of ²³⁸Pu/ ²³⁹Pu/ ²⁴⁰Pu/ ²⁴¹Pu/ ²⁴²Pu. Four protective TRISO layers consist of porous carbon buffer (C), inner pyrolytic carbon (iPyC), silicon carbide (SiC), and outer pyrolytic carbon (oPyC). These layers effectively retain the radioactive fission products up to the temperature of 1600 °C. Figure 3 shows a schematic view of a fuel pebble and a TRISO particle. Fuel pebble and coated fuel particles with UO₂, PuO₂, and (Th, U)O₂ kernels have the same design and specifications. Detailed specifications are described in tab. 1.

CALCULATION MODEL

Calculations of kinetic parameters of pebble bed reactor were performed using Monte Carlo transport code MCNP6 and continuous energy nuclear data library ENDF/B-VII. In the modeling of a pebble bed reactor, special attention must be paid to taking into account the double heterogeneity in the core region. It consists of TRISO fuel particles in the fueled zone of the pebble and pebble lattice containing fuel and moderator pebbles in the reactor core.

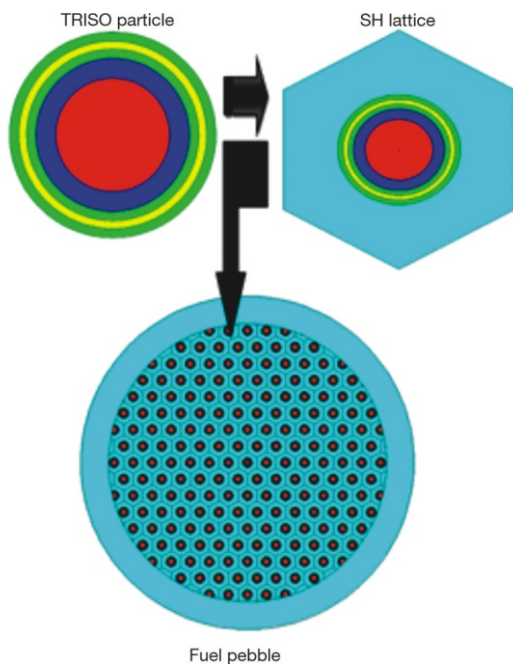
The core modeling is starting from the modeling of the TRISO particle using a simple hexagonal lattice. This lattice has a hexagonal pitch of 0.171456 cm. Next, the fuel pebble is modeled by constructing a regu-

Table 1. Fuel pebble and coated particle specifications

Fuel pebble	
Diameter [cm]	6
Radius of the fueled zone [cm]	2.5
Thickness of graphite shell [cm]	0.5
Density of graphite shell [gcm^{-3}]	1.75
Impurity of natural boron in graphite matrix [ppm*]	0.5
Density of graphite matrix [gcm^{-3}]	1.75
Impurity of natural boron in graphite shell [ppm]	0.5
Number of coated particles in pebble	15000
Mass of fuel per pebble [g]	10.210
Coated particle	
Kernel	
Radius [cm]	0.025
Density [gcm^{-3}]	10.4
Impurity of natural boron in the kernel [ppm]	0.5
Coatings	
Material	C/iPyC/SiC/oPyC
Thickness [cm]	0.095/0.04/0.035/0.04
Density [gcm^{-3}]	1.05/1.9/3.18/1.9
Packing fraction of coated particle [%]	9.043

*parts per million

lar array of lattice particles within the fueled zone of the pebble. Dispersing the 15 000 TRISO particles in each repetitively structured fuel pebble will result in the TRISO particles being cut in the boundary between the fueled zone and graphite shell. However, this condition may be considered negligible due to the insignificant impact it imposes on the calculation results. The MCNP6 model of fuel pebble is illustrated in fig. 4. The

**Figure 4. The MCNP6 model of fuel pebble****Table 2. Isotopic composition of TRISO particle**

Kernel UO_2		Kernel (Th, U) O_2	
^{235}U	$4.32074 \cdot 10^{-2}$	^{232}Th	$2.07618 \cdot 10^{-2}$
^{238}U	$1.89195 \cdot 10^{-3}$	^{233}U	$2.94769 \cdot 10^{-3}$
O	$4.64805 \cdot 10^{-2}$	O	$4.74189 \cdot 10^{-2}$
^{10}B	$1.14694 \cdot 10^{-7}$	^{10}B	$1.14694 \cdot 10^{-7}$
^{11}B	$4.64570 \cdot 10^{-7}$	^{11}B	$4.64570 \cdot 10^{-7}$
Kernel PuO_2		Buffer	
^{238}Pu	$6.01178 \cdot 10^{-4}$	^{12}C	$5.26449 \cdot 10^{-2}$
^{239}Pu	$1.24470 \cdot 10^{-2}$	iPyC/oPyC	
^{240}Pu	$5.44599 \cdot 10^{-3}$	^{12}C	$9.52621 \cdot 10^{-2}$
^{241}Pu	$3.00965 \cdot 10^{-3}$	SiC	
^{242}Pu	$1.54539 \cdot 10^{-3}$	^{28}Si	$4.39872 \cdot 10^{-2}$
O	$4.60983 \cdot 10^{-2}$	^{29}Si	$2.24780 \cdot 10^{-3}$
^{10}B	$1.14694 \cdot 10^{-7}$	^{30}Si	$1.48899 \cdot 10^{-3}$
^{11}B	$4.64570 \cdot 10^{-7}$	^{12}C	$4.77240 \cdot 10^{-2}$

Table 3. Isotopic composition of graphite matrix and graphite shell

Graphite matrix		Graphite shell	
^{12}C	$8.77414 \cdot 10^{-2}$	^{12}C	$8.77414 \cdot 10^{-2}$
^{10}B	$9.64977 \cdot 10^{-9}$	^{10}B	$9.64977 \cdot 10^{-9}$
^{11}B	$3.90864 \cdot 10^{-8}$	^{11}B	$3.90864 \cdot 10^{-8}$

isotopic composition of TRISO coated fuel particle (in atom per barn per cm; 1 barn = 10^{-28} m^2) is listed in tab. 2. The identical isotopic composition of graphite matrix and graphite shell (in atom per barn per cm) is listed in tab. 3.

The reactor core filled with thousands of pebbles was modeled using body centered-cubic (BCC) lattice with repetitive structures. This lattice is the most representative with a core characterized by fuel and moderator pebbles with the ratio of 1:1 due to the BCC lattice consisting of two pebbles. In addition, despite the pebbles arrangement on the pebble bed core is expected to approach the hexagonal close-packed (HCP) lattice, the BCC lattice is more often a choice, thanks to its ability to provide packing size typically found in pebble bed reactors. The lattice pitch of 7.224957 cm was obtained from the correlation between the pebble volume in the lattice and the specified packing fraction of 0.60.

The appearance of a number of clipped pebbles on the core wall surface as a result of the use of repetitive structures, called partial pebbles, was corrected by applying an exclusive zone of 1.5 cm thick helium around the reactor core. This is undertaken to compensate for the partial pebbles which may be affecting the calculation accuracy. Core components and structures, such as axial and radial reflectors, etc., were modeled in a simpler way. A detailed description of this procedure was first introduced by Lebenhaft [19] and found in several publications [20-28]. The whole facility modeling of HTR-Proteus is illustrated in fig. 5. The isotopic composition of moderator pebble (in atom per barn per cm) is given in

Figure 5. The MCNP6 model for HTR-Proteus

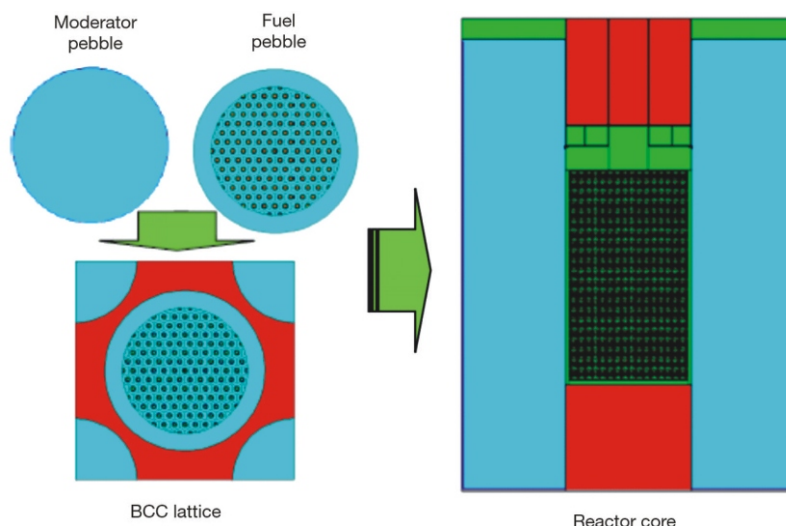


Table 4. Isotopic composition of moderator pebble

Moderator pebble	
¹² C	8.38302 10 ⁻²
¹⁰ B	2.40326 10 ⁻⁸
¹¹ B	9.73442 10 ⁻⁸

Table 5. Isotopic composition of axial and radial reflectors

Axial reflector		Radial reflector	
¹² C	8.61000 10 ⁻²	¹² C	8.84000 10 ⁻²
¹⁰ B	9.00000 10 ⁻⁹	¹⁰ B	9.20000 10 ⁻⁹
¹¹ B	3.60000 10 ⁻⁸	¹¹ B	3.70000 10 ⁻⁸

tab. 4. The isotopic composition of axial and radial reflectors (in atom per barn per cm) is presented in tab. 5.

RESULTS AND DISCUSSION

The most important kinetic parameters of a reactor consist of the effective delayed neutron fraction β_{eff} , prompt neutron lifetime ℓ , and mean generation time [29]. These parameters were analyzed in this study. The core multiplication factor k_{eff} was also analyzed since the calculation of kinetic parameters is strongly connected to criticality calculations. To run the criticality problems, KCODE and KSRC cards are required in addition to the geometry description and material cards. The KSRC card which specifies the location of

the initial spatial fission point was defined at the center of the fuel kernel and the KCODE card which determines the reactor multiplication factor was simulated with 25 000 particles per neutron life cycle. A total of 5 million neutron histories were used with discarding of the first 50 cycles of 250 cycles before averaging k_{eff} . The calculation of kinetic parameters was conducted by activating the KOPTS card in the MCNP6 input data. The control rods were placed in a fully withdrawn position.

The core has been modeled with different fuel compositions and different temperatures to examine their effects on the core multiplication factor k_{eff} and its kinetic parameters. Calculated k_{eff} results of the HTR-Proteus reactor are presented in tab. 6. From this table, it can be observed that the increase in fuel temperature T_F , moderator temperature T_M , and reflector temperature T_R simultaneously causes a decrease in the k_{eff} value. The largest decrease in k_{eff} value was found in the core with UO_2 fuel, followed by the core with $(\text{Th}, \text{U})\text{O}_2$ and PuO_2 fuels. The calculation results of the temperature reactivity coefficient are calculated from the data in tab. 6 and presented in tab. 7 show that within a temperature range of 900 K-1200 K, the value of the total core temperature reactivity coefficient of UO_2 and $(\text{Th}, \text{U})\text{O}_2$ is the most negative while in the temperature range of 1200 K-2500 K, the position was taken over by the PuO_2 core. This means that at operating temperature, the HTR-Proteus core has an adequate safety factor.

Table 6. Core multiplication factor k_{eff}

Temperature [K]	UO_2	$(\text{Th}, \text{U})\text{O}_2$	PuO_2
$T_F = 293, T_M = 293, T_R = 293$	1.06737 0.00041	1.06778 0.00035	1.06749 0.00034
$T_F = 600, T_M = 600, T_R = 600$	1.04472 0.00035	1.04483 0.00037	1.07228 0.00033
$T_F = 900, T_M = 900, T_R = 900$	1.02588 0.00038	1.02945 0.00033	1.06774 0.00034
$T_F = 1200, T_M = 1200, T_R = 1200$	0.99548 0.00037	1.00739 0.00037	1.05368 0.00038
$T_F = 2500, T_M = 2500, T_R = 2500$	0.93593 0.00037	0.97874 0.00034	0.98223 0.00033

Table 7. Total temperature coefficient of reactivity ($k k^{-1}K^{-1}$)

Temperature range [K]	UO ₂	(Th, U)O ₂	PuO ₂
293-600	-6.6163 10 ⁻⁵	-6.70065 10 ⁻⁵	-1.36309 10 ⁻⁵
600-900	-5.85954 10 ⁻⁵	-4.76633 10 ⁻⁵	-1.32179 10 ⁻⁵
900-1200	-9.92255 10 ⁻⁵	-7.09057 10 ⁻⁵	-4.16572 10 ⁻⁵
1200-2500	-4.91657 10 ⁻⁵	-2.2352 10 ⁻⁵	-5.31052 10 ⁻⁵

The k_{eff} calculation results and kinetic parameters as a function of fuel temperature are summarized in tab. 8. In this case, the fuel temperature is varied while the moderator and reflector are maintained at a temperature of 293 K. Similar to tab. 7, tab. 8 shows that the increase in fuel temperature caused a significant decrease in the k_{eff} value and the largest one was found in the core with UO₂ fuel followed by (Th, U)O₂ and PuO₂. The decrease in the k_{eff} value is caused by the Doppler broadening effect in the resonance region of the fuel which affects the amount of neutron absorption by isotopes in the fuel. Compared with the value of the reactivity coefficient in tab. 7, the reactivity effect of fuel temperature, tab. 9, appears to be more negative, especially for UO₂ and (Th, U)O₂ cores. The same thing was experienced by the PuO₂ core but at a temperature range of less than 900 K. From this observation, we could say that the negative value on core temperature reactivity is affected dominantly by the Doppler broadening effect of fuel temperature.

Table 8 confirms that the change in fuel temperature has a significant effect on the ℓ and β_{eff} but this change hardly affects the value of the β_{eff} . The increase in fuel temperature causes the value of ℓ and β_{eff} of the UO₂ core and (Th, U)O₂ core to increase by 1.32-8.79 % and 1.35-6.20 %, respectively. Different things are experienced by the PuO₂ core, the increase in fuel temperature actually decreases the value of ℓ even though the decrease is still below 0.25 %, while the value of the β_{eff} still increases

Table 9. Fuel temperature coefficient of reactivity ($k k^{-1}K^{-1}$)

Temperature range [K]	UO ₂	(Th, U)O ₂	PuO ₂
293-600	-8.65901 10 ⁻⁵	-9.10308 10 ⁻⁵	-2.61194 10 ⁻⁵
600-900	-6.89657 10 ⁻⁵	-6.03986 10 ⁻⁵	-2.23847 10 ⁻⁵
900-1200	-1.07223 10 ⁻⁴	-1.05196 10 ⁻⁴	-3.26238 10 ⁻⁵
1200-2500	-4.93204 10 ⁻⁵	-3.83392 10 ⁻⁵	-1.98315 10 ⁻⁵

from 0.77-3.11 %. Looking back at tab. 8, it can be found that the UO₂ core is easier to control because the β_{eff} value is the largest one, in contrast to (Th, U)O₂ and PuO₂ which are almost half of the UO₂ fuel system.

The effect of the temperature moderator on kinetic parameters is summarized in tab. 10. The moderator temperature was varied while the fuel and reflector temperatures were kept constant at 1200 K and 293 K, respectively. Table 10 shows that increasing the graphite moderator temperature causes the k_{eff} value to decrease, but not as significant as increasing fuel temperature. The k_{eff} value decreases slightly as the moderator temperature increases because of an increase in neutron absorption from materials other than fuels. The largest decrease in k_{eff} was experienced by the UO₂ core, followed by the (Th, U)O₂ and PuO₂ cores. Table 10 represents a recurring trend as the moderator temperature increases for the ℓ and β_{eff} of UO₂ and (Th, U)O₂ cores, which increase within the range 0.70-2.23 % and 0.58-0.67 %, respectively. The same trend is also experienced by the PuO₂ core, with the increase in fuel temperature actually decreasing the ℓ value even though the decrease is very small (<0.15 %), while the value of the β_{eff} increases by 0.49 % at a moderator temperature of 1200 K and decreases by 0.33-0.78 % at a moderator temperature of 600 K and 900 K. Similar to tab. 8, the β_{eff} value does not change as the moderator temperature increases. Compared to the total temperature coefficient of reactivity ($k k^{-1}K^{-1}$) in tab. 7 and fuel temper-

Table 8. Effect of fuel temperature T_F on kinetic parameters ($T_M = 293$ K, $T_R = 293$ K)

Fuel temperature T_F [K]	k_{eff}	ℓ [s]	β_{eff}
UO ₂	293	1.06737 0.00041	3.2507 10 ⁻³ 1.5126 10 ⁻⁶ 1.6789 10 ⁻³ 1.2600 10 ⁻⁵ 0.00665 0.00038
	600	1.03792 0.00038	3.3108 10 ⁻³ 1.4263 10 ⁻⁶ 1.7710 10 ⁻³ 1.3080 10 ⁻⁵ 0.00629 0.00039
	900	1.01610 0.00038	3.3545 10 ⁻³ 1.5732 10 ⁻⁶ 1.8369 10 ⁻³ 1.3820 10 ⁻⁵ 0.00663 0.00040
	1200	0.98394 0.00039	3.4364 10 ⁻³ 1.4784 10 ⁻⁶ 1.9507 10 ⁻³ 1.5470 10 ⁻⁵ 0.00620 0.00038
	2500	0.92555 0.00033	3.5639 10 ⁻³ 1.4588 10 ⁻⁶ 2.1222 10 ⁻³ 1.6860 10 ⁻⁵ 0.00639 0.00039
(Th,U)O ₂	293	1.06778 0.00035	3.6369 10 ⁻³ 1.4876 10 ⁻⁶ 1.8651 10 ⁻³ 1.3890 10 ⁻⁵ 0.00369 0.00029
	600	1.03684 0.00037	3.7054 10 ⁻³ 1.4998 10 ⁻⁶ 1.9249 10 ⁻³ 1.4510 10 ⁻⁵ 0.00345 0.00027
	900	1.01772 0.00036	3.7553 10 ⁻³ 1.5723 10 ⁻⁶ 1.9621 10 ⁻³ 1.5160 10 ⁻⁵ 0.00274 0.00025
	1200	0.98605 0.00037	3.8476 10 ⁻³ 1.5206 10 ⁻⁶ 2.0629 10 ⁻³ 1.6480 10 ⁻⁵ 0.00299 0.00028
	2500	0.93986 0.00038	3.9776 10 ⁻³ 1.6016 10 ⁻⁶ 2.1909 10 ⁻³ 1.8360 10 ⁻⁵ 0.00299 0.00029
PuO ₂	293	1.06749 0.00034	2.0983 10 ⁻³ 1.2841 10 ⁻⁶ 9.6555 10 ⁻⁴ 8.9429 10 ⁻⁶ 0.00357 0.00028
	600	1.05843 0.00038	2.0976 10 ⁻³ 1.2887 10 ⁻⁶ 9.7797 10 ⁻⁴ 9.5914 10 ⁻⁶ 0.00285 0.00024
	900	1.05096 0.00033	2.0929 10 ⁻³ 1.2343 10 ⁻⁶ 9.8606 10 ⁻⁴ 9.4730 10 ⁻⁶ 0.00334 0.00027
	1200	1.04026 0.00035	2.0901 10 ⁻³ 1.3359 10 ⁻⁶ 9.9368 10 ⁻⁴ 9.3932 10 ⁻⁶ 0.00280 0.00022
	2500	1.01309 0.00036	2.0850 10 ⁻³ 1.3816 10 ⁻⁶ 1.0246 10 ⁻³ 9.9400 10 ⁻⁶ 0.00299 0.00025

Table 10. Effect of moderator temperature T_M on kinetic parameters ($T_F = 1200$ K, $T_R = 293$ K)

Moderator temperature T_M [K]		k_{eff}		ℓ [s]		Λ [s]		β_{eff}	
UO ₂	293	0.98394	0.00039	3.4364 10 ⁻³	1.4784 10 ⁻⁶	1.9507 10 ⁻³	1.5470 10 ⁻⁵	0.00620	0.00038
	600	0.97396	0.00035	3.4633 10 ⁻³	1.4965 10 ⁻⁶	1.9942 10 ⁻³	1.5550 10 ⁻⁵	0.00726	0.00043
	900	0.96531	0.00037	3.4876 10 ⁻³	1.4458 10 ⁻⁶	1.9987 10 ⁻³	1.6150 10 ⁻⁵	0.00626	0.00040
	1200	0.94935	0.00038	3.5342 10 ⁻³	1.3584 10 ⁻⁶	2.0333 10 ⁻³	1.6350 10 ⁻⁵	0.00710	0.00043
(Th,U)O ₂	293	0.98605	0.00037	3.8476 10 ⁻³	1.5206 10 ⁻⁶	2.0627 10 ⁻³	1.6480 10 ⁻⁵	0.00299	0.00028
	600	0.97635	0.00036	3.8732 10 ⁻³	1.4584 10 ⁻⁶	2.0629 10 ⁻³	1.6330 10 ⁻⁵	0.00303	0.00027
	900	0.96861	0.00037	3.8955 10 ⁻³	1.4583 10 ⁻⁶	2.0765 10 ⁻³	1.6800 10 ⁻⁵	0.00352	0.00033
	1200	0.95427	0.00037	3.9360 10 ⁻³	1.4482 10 ⁻⁶	2.0833 10 ⁻³	1.6570 10 ⁻⁵	0.00338	0.00031
PuO ₂	293	1.04026	0.00035	2.0901 10 ⁻³	1.3359 10 ⁻⁶	9.9368 10 ⁻⁴	9.3932 10 ⁻⁶	0.00280	0.00022
	600	1.03684	0.00036	2.0897 10 ⁻³	1.2734 10 ⁻⁶	9.8594 10 ⁻⁴	9.3016 10 ⁻⁶	0.00292	0.00024
	900	1.03365	0.00034	2.0875 10 ⁻³	1.2762 10 ⁻⁶	9.8271 10 ⁻⁴	9.4513 10 ⁻⁶	0.00309±0.00024	
	1200	1.02652	0.00036	2.0848 10 ⁻³	1.3670 10 ⁻⁶	9.8749 10 ⁻⁴	9.7416 10 ⁻⁶	0.00374	0.00028

Table 11. Moderator temperature coefficient of reactivity (k k⁻¹K⁻¹)

Temperature range [K]	UO ₂	(Th, U)O ₂	PuO ₂
293-600	-3.39221 10 ⁻⁵	-3.28193 10 ⁻⁵	-1.03284 10 ⁻⁵
600-900	-3.06681 10 ⁻⁵	-2.72813 10 ⁻⁵	-9.92166 10 ⁻⁶
900-1200	-5.80522 10 ⁻⁵	-5.17139 10 ⁻⁵	-2.23989 10 ⁻⁵

ature coefficient of reactivity (k k⁻¹K⁻¹) values in tab. 9, the moderator temperature coefficient of reactivity (k k⁻¹K⁻¹) in tab. 11 is slightly smaller for all three HTR-Proteus cores considered.

The effect of reflector temperature T_R on kinetic parameters ($T_F = 1200$ K, $T_M = 1200$ K) is summarized in tab. 12. Unlike other previously mentioned cases, when the reflector temperature increases, the k_{eff} value increases. The increase in k_{eff} value is quite significant compared to the decrease of the k_{eff} value when the moderator temperature is increased. Therefore, the reflector temperature coefficient of reactivity is positive, as shown in tab. 13. This means that the number of neutrons coming out of the reactor is reduced which is most likely due to the backscattering of neutrons into the reactor core that occurs in the reflector. Because

Table 13. Reflector temperature coefficient of reactivity RTC (k k⁻¹K⁻¹)

Temperature range [K]	UO ₂	(Th, U)O ₂	PuO ₂
293-600	9.32431 10 ⁻⁵	9.85160 10 ⁻⁵	5.73674 10 ⁻⁵
600-900	2.89788 10 ⁻⁵	3.59327 10 ⁻⁵	1.66267 10 ⁻⁵
900-1200	3.83083 10 ⁻⁵	4.74434 10 ⁻⁵	8.36861 10 ⁻⁶

the material used as neutron moderator and reflector is the same graphite material, it can be said that this backscattering phenomenon can also occur inside the reactor core. Increasing the moderator temperature causes the k_{eff} value to increase due to the increasing number of moderated neutrons, but on the other hand, the effect of neutron absorption from non-fuel materials whose temperature increases due to the Doppler effect is predicted to be more dominant when inside the reactor core, different from the radial and axial reflector that positioned on the edge of the core.

The UO₂ and (Th, U)O₂ cores have a higher reflector temperature coefficient of reactivity than PuO₂ core because there is a greater increase in k_{eff} . The calculation results of the kinetic parameters shown in tab. 12 give the impression that the value of the ℓ and Λ are

Table 12. Effect of reflector temperature T_R on kinetic parameters ($T_F = 1200$ K, $T_M = 1200$ K)

Reflector temperature T_R [K]		k_{eff}		ℓ [s]		Λ [s]		β_{eff}	
UO ₂	293	0.94935	0.00038	3.5342 10 ⁻³	1.3584 10 ⁻⁶	2.0333 10 ⁻³	1.6350 10 ⁻⁵	0.00710	0.00043
	600	0.97587	0.00035	2.9834 10 ⁻³	1.3754 10 ⁻⁶	1.7763 10 ⁻³	1.3180 10 ⁻⁵	0.00668	0.00042
	900	0.98422	0.00038	2.7518 10 ⁻³	1.1517 10 ⁻⁶	1.6795 10 ⁻³	1.1970 10 ⁻⁵	0.00752	0.00046
	1200	0.99548	0.00037	2.4433 10 ⁻³	1.0271 10 ⁻⁶	1.5508 10 ⁻³	1.1030 10 ⁻⁵	0.00717	0.00043
(Th,U)O ₂	293	0.95427	0.00037	3.9360 10 ⁻³	1.4876 10 ⁻⁶	2.0833 10 ⁻³	1.6570 10 ⁻⁵	0.00338	0.00031
	600	0.98263	0.00034	3.3424 10 ⁻³	1.3384 10 ⁻⁶	1.8855 10 ⁻³	1.4510 10 ⁻⁵	0.00260	0.00025
	900	0.99315	0.00034	3.0898 10 ⁻³	1.2130 10 ⁻⁶	1.97574 10 ⁻³	1.2860 10 ⁻⁵	0.00299	0.00028
	1200	1.00739	0.00037	2.7523 10 ⁻³	1.1410 10 ⁻⁶	1.6099 10 ⁻³	1.1460 10 ⁻⁵	0.00317	0.00029
PuO ₂	293	1.02652	0.00036	2.0848 10 ⁻³	1.3670 10 ⁻⁶	9.8749 10 ⁻⁴	9.7416 10 ⁻⁶	0.00374	0.00028
	600	1.04542	0.00033	1.6812 10 ⁻³	1.0354 10 ⁻⁶	8.3326 10 ⁻⁴	7.6371 10 ⁻⁶	0.00298	0.00024
	900	1.05090	0.00037	1.5180 10 ⁻³	1.0616 10 ⁻⁶	7.6837 10 ⁻⁴	6.8161 10 ⁻⁶	0.00320	0.00026
	1200	1.05368	0.00038	1.3032 10 ⁻³	8.6296 10 ⁻⁷	6.7693 10 ⁻⁴	5.8807 10 ⁻⁶	0.00301	0.00023

decreasing while reflector temperature is increasing for all cores. This value is on the opposite trend of the ℓ and β_{eff} when the fuel and moderator temperatures increase. More specifically, the ℓ and β_{eff} of the PuO_2 core are also decreased as the moderator temperature increase. Again, it can be found that the UO_2 core is easier to control because its β_{eff} value is greatest when the reflector temperature increases. The β_{eff} values of (Th, U) O_2 and PuO_2 cores are almost half of the UO_2 core β_{eff} values.

Changes in the ℓ and β_{eff} due to changes in temperature of the fuel, moderator and reflector may be caused by factors related to neutron moderation and neutron absorption by fissile and fertile materials in the core. The β_{eff} value is very specific and only depends on the isotope used as a fissile and fertile material. That is why changes in temperature of the fuel moderator, and reflector do not have much effect on the β_{eff} value because the composition of the fissile and fertile material is practically the same or does not change as the temperature changes. For the (Th, U) O_2 core, the β_{eff} value obtained is dominated by the presence of ^{233}U while for the UO_2 and PuO_2 cores, the β_{eff} values are more influenced by the ^{235}U , and ^{239}Pu isotopes, respectively. If the fuel composition of the core is different, especially the fissile material, the β_{eff} will also be different.

CONCLUSION

A study on the characteristics of kinetic parameters for pebble bed reactor using HTR-Proteus has been conducted. A series of calculations with various temperatures were performed by using the Monte Carlo transport code MCNP6 and the continuous energy nuclear data library ENDF/B-VII. The calculation results show that the negative value on core temperature reactivity is affected dominantly by the Doppler broadening effect of fuel temperature. The moderator temperature coefficient is slightly smaller for all three HTR-Proteus cores considered. UO_2 and (Th, U) O_2 cores have a higher reflector temperature coefficient of reactivity than PuO_2 core. Changes in the ℓ and β_{eff} due to changes in temperature of the fuel, moderator and reflector may be caused by factors related to neutron moderation and neutron absorption by fissile and fertile materials in the core. For the (Th, U) O_2 core, the β_{eff} value obtained is dominated by the presence of ^{233}U while for the UO_2 and PuO_2 cores, the β_{eff} values are more influenced by the ^{235}U , and ^{239}Pu isotopes, respectively. The UO_2 core is easier to control because the β_{eff} value is the largest one, in contrast to (Th, U) O_2 and PuO_2 which are almost half of the UO_2 fuel system. It can be concluded, that changing temperature not only affects the temperature coefficient of reactivity but also kinetic parameters as an inherent safety feature of a pebble-bed reactor.

AUTHOR'S CONTRIBUTIONS

All authors contributed equally to this manuscript.

ACKNOWLEDGMENT

The authors express their gratitude to Prof. Surian Pinem, M.Sc. and Dr. Anis Rohanda for providing motivation and encouragement in this work. The authors are also very grateful to all colleagues in the Research Group of Nuclear Reactor Design and Physics for their kind help and moral support. This research was funded by the Government of the Republic of Indonesia through Rumah Program HITN-ORTN 2022.

REFERENCES

- [1] ***, The International Renewable Energy Agency (IRENA), Global Energy Transformation: A roadmap to 2050, International Renewable Energy Agency, Abu Dhabi, 2018
- [2] Arostegui, D. A., Holt, M., Advanced Nuclear Reactors: Technology Overview and Current Issues, Congressional Research Service, April 18, 2019, R45706
- [3] Boer, B., Optimized Core Design and Fuel Management of a Pebble-Bed Type Nuclear Reactor, Ph. D Thesis, Technische Universiteit Delft, 2009, January
- [4] Zuhair, *et al.*, The Implication of Thorium Fraction on Neutronic Parameters of Pebble Bed Reactor, *Kuwait Journal of Science*, 48 (2021), 3, pp. 1-16
- [5] Sahin, H. M., Erol, O., Utilization of Thorium in a Gas Turbine – Modular Helium Reactor with Alternative Fuels, *Energy Conversion and Management*, 53 (2012), 1, pp. 224-229
- [6] Zuhair, *et al.*, Investigation on Criticality and Burnup Performance of Pebble Bed Reactor with Thorium-Based Nuclear Fuel, *Philippine Journal of Science*, 150 (2021), 3, pp. 1019-1027
- [7] Zuhair, *et al.*, Study on the Characteristics of Effective Delayed Neutron Fraction (β_{eff}) for Pebble-Bed Reactor with Plutonium Fuel, *Iranian Journal of Science and Technology, Transactions A: Science*, 43 (2019), 6, pp. 3037-3045
- [8] Acir, A., Coskun, H., Neutronic Analysis of the PBMR-400 Full Core Using Thorium Fuel Mixed with Plutonium or Minor Actinides, *Annals of Nuclear Energy*, 48 (2012), Oct., pp. 45-50
- [9] Zuhair, *et al.*, Study on Characteristic of Temperature Coefficient of Reactivity for Plutonium Core of Pebbled Bed Reactor, IOP Conf. Series: *Journal of Physics*, (2018), Conf. Series 962
- [10] Ho, H. Q., Obara, T., Design Concept for A Small Pebble Bed Reactor with ROX Fuel, *Annals of Nuclear Energy*, 87 (2016), 2, pp. 471-478
- [11] Dibyo, S., *et al.*, Transient Calculation on Triga 2000 of Plate-Type Fuel Element Using RELAP5, EUREKA2/RR, and MTR-DYN Codes, *Nucl Technol Radiat*, 36 (2021), 3, pp. 211-218
- [12] Williams, T., LEU-HTR PROTEUS: Configuration and Critical Balances for the Cores of the HTR-PROTEUS Experimental Programme, Paul Scherrer Institute, 1996, TM-41-95-18

- [13] Goorley, J. T., et al., Initial MCNP6 Release Overview – MCNP6 Version 1.0, Los Alamos National Laboratory, 2013, LA-UR-13-22934
- [14] Chadwick, M. B., et al., ENDF/B-VII: Next Generation Evaluated Nuclear Data Library for Nuclear Science and Technology, *Nuclear Data Sheets*, 107 (2006), 12, pp. 2931-3060
- [15] Bess, J. D., et al., Benchmark Evaluation of HTR-PROTEUS Pebble Bed Experimental Program, *Nuclear Science and Engineering*, 178 (2014), 3, pp. 387-400
- [16] Williams, T., et al., Critical Experiments and Reactor Physics Calculations for Low-Enriched High Temperature Gas Cooled Reactors, IAEA-TECDOC-1249, 2001
- [17] Mathews, D., Chawla, R., LEU-HTR PROTEUS Computational Benchmark Specifications, Paul Scherrer Institute, Report TM-41-90-32, 1990
- [18] Setiadipura, T., Irwanto, D., Zuhair, Preliminary Neutronic Design of High Burnup OTTO Cycle Pebble Bed Reactor, *Atom Indonesia* 41 (2015), 1, pp. 7-15
- [19] Lebenhaft, J. L., MCNP4B Modeling of Pebble-Bed Reactors, MSNE thesis, Massachusetts Institute of Technology, Massachusetts, USA, 2001
- [20] Alzamly, M. A., et al., Burnup Analysis for HTR-10 Reactor Core Loaded with Uranium and Thorium Oxide, *Nuclear Engineering and Technology*, 52 (2020), 4, pp. 674-680
- [21] Zuhair, et al., Study on MCNP6 Model in the Calculation of Kinetic Parameters for Pebble Bed Reactor, *Acta Polytechnica*, 60 (2020), 2, pp. 175-184
- [22] Zuhair, et al., The Effects of Fuel Type on Control Rod Reactivity of Pebble-Bed Reactor, *Nukleonika*, 64 (2019), 4, pp. 131-138
- [23] Hosseini, S. A., Athari-Allaf, M., Effects of the Wallpaper Fuel Design on the Neutronic Behavior of the HTR-10, *Kerntechnik*, 81 (2016), 6, pp. 627-633
- [24] Zuhair, et al., Study on Control Rod Reactivity of Small Pebble Bed Reactor with Wallpaper Fuel Design, IOP Conf. Series: *Journal of Physics*, (2021), Conf. Series 1772
- [25] Zuhair, et al., Neutronic Effect of Utilizing TRIZO Particles on Core Characteristics of Experimental Power Reactor, AIP Conference Proceedings 2180, 020005, Padang, Indonesia (2019), <https://doi.org/10.1063/1.5135509>
- [26] Hosseini, S. A., Athari-Allaf, M., Implementation and Benchmarking of ENDF/B-VII based Library for PBM Reactor Analysis with MCNP4c, *Progress in Nuclear Energy*, 60 (2012), pp. 27-30
- [27] Zuhair, et al., Study on MOX Core Characteristics of Experimental Power Reactor using MCNP6 Code, IOP Conf. Series: *Journal of Physics*, (2019), Conf. Series 1198
- [28] Zuhair, et al., The Effects of Applying Silicon Carbide Coating on Core Reactivity of Pebble-Bed HTR in Water Ingress Accident, *Kerntechnik*, 82 (2017), 1, pp. 92-97
- [29] Muhammad, A., et al., Kinetic Parameters Study based on Burn-up for Improving the Performance of Research Reactor Equilibrium Core, *Nucl Technol Radiat*, 29 (2014), 4, pp. 253-258

Received on June 3, 2022

Accepted on August 31, 2022

ЗУХАИР, Вахид ЛУТФИ, СРИЈОНО, СУВОТО, Топан СЕТИАДИПУРА

ПРОУЧАВАЊЕ КАРАКТЕРИСТИКА КИНЕТИЧКИХ ПАРАМЕТАРА РЕАКТОРА СА СВЕРНИМ ГОРИВОМ КОРИШЋЕЊЕМ HTR-PROTEUS ПОСТРОЈЕЊА

Инхерентна сигурност карактеристика реактора са сверним горивом може се уочити из његових кинетичких параметара. Такође, брига за правилно моделовање кинетике реактора потребно је ради сигурног рада током нормалних и прелазних режима. Овај рад има за циљ да истражи карактеристике кинетичких параметара реактора са сверним горивом коришћењем HTR-PROTEUS постројења. Серија прорачуна спроведена је коришћењем MCNP6 кода и библиотеке ENDF/B-VII.1. Резултати прорачуна показују да на негативну вредност температурне реактивности језгра доминантно утиче ефекат Доплеровог ширења. Промптни животни век неутрона и средње време генерисања мало се мењају услед повећања температуре горива, модератора и рефлектора, који утичу на модерацију и апсорпцију неутрона у овом делу реактора. За језгра (Th, U)O₂, UO₂ и PuO₂, ефективне вредности фракције закаснелих неутрона више су под утицајем ²³³U, ²³⁵U и ²³⁹Pu, респективно. У погледу стабилности током уношења реактивности, језгро UO₂ је стабилније и лакше га је контролисати јер је вредност његове фракција закаснелих неутрона највећа у поређењу са (Th, U)O₂ и PuO₂ језгрима. Може се закључити да се промена температуре мора контролисати јер не утиче само на реактивност већ и на кинетичке параметре као део тока својствених сигурносних карактеристика реактора са сверним горивом.

Кључне речи: кинетички параметар, реактор са сверним горивом, HTR-PROTEUS, MCNP6, ENDF/B-VII